THE JOURNAL OF PHYSICAL CHEMISTRY B

ARTICLE

pubs.acs.org/JPCB

Low Energy Electron Attachment to the Adenosine Site of DNA

Jiande Gu,*[,†,‡] Jing Wang,[‡] and Jerzy Leszczynski*[,‡]

[†]Drug Design & Discovery Center, State Key Laboratory of Drug Research, Shanghai Institute of Materia Medica, Shanghai Institutes for Biological Sciences, CAS Shanghai, 201203 P. R. China

[‡]Interdisciplinary Nanotoxicity Center, Department of Chemistry and Biochemistry, Jackson State University, Jackson, Mississippi 39217, United States

ABSTRACT: To evaluate the role of adenosine in low energy electron (LEE) induced DNA strand breaks, theoretical investigations of the LEE attachment induced C−O σ bonds and *N*-glycosidic bond breaking of 2′-deoxyadenosine-3′,5′-diphosphate (3′,5′-dAMP) were performed at the B3LYP/DZP++ level of theory. The results indicate that, although adenine-rich oligonucleotides are capable of capturing the near 0 eV electron to form the electronically stable radical anions in the gas phase, it is unlikely to undergo either C−O σ bond cleavage or the glycosidic processes due to the low electron detachment energy (VDE) of 3′,5′-dADP$^-$ unit (0.26 eV). Instead, these radical anions should directly yield an electron detachment product in the gas phase. In the presence of polarizable surroundings, due to the large increase of the electron detachment energy (VDE increases to 1.59 eV), the adenine-centered radical anions could directly lead to strand breaks in the adenine-rich DNA single strands through either σ bond or *N*-glycosidic bond breaking. The values of activation energy for rupture of the $C_{5'}-O_{5'}$ σ bond (22.5 kcal/mol), the *N*-glycosidic bond (20.2 kcal/mol), and the $C_{3'}-O_{3'}$ σ bond (13.2 kcal/mol) indicate that $C_{3'}-O_{3'}$ σ bond breaking should dominate. Moreover, along with the previous research, the predicted ratio of the activation energy barrier of the $C_{5'}-O_{5'}$ σ bond breakage in 3′,5′-dXDP$^-$ (X = G, A, T) partly explains the observation in the femtosecond time-resolved laser spectroscopic experiment that the $C_{5'}-O_{5'}$ σ bond breaking only occurs in dGMP$^-$ and dTMP$^-$ not in dAMP$^-$. This study completes the series of LEE-induced DNA single strand breaking investigations for the four basic DNA units 3′,5′-dXDP (X = G, A, T, C). The obtained results are vital for elucidating the experimental observations. Combined with the previous studies, the information revealed in this study is crucial for understanding the mechanisms of the interactions between the LEE and the DNA stands.

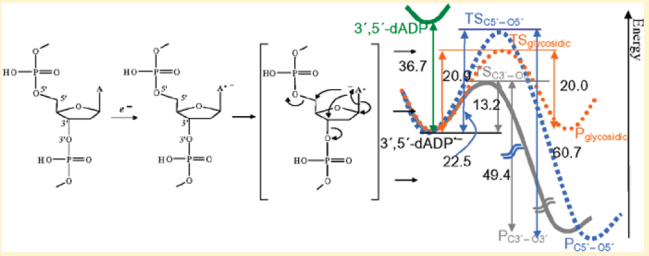

INTRODUCTION

Low energy electron (LEE) attachment to DNA has attracted much attention since the observation of the LEE induced DNA strand rupture.[1] Due to the fact that low energy electrons are produced in abundance during ionizing radiation,[2,3] a detailed understanding of this LEE-induced DNA damage is of crucial importance for the advancement of radiation biology. Both experimental investigations and theoretical studies of different DNA fragment models suggest that LEE attachment to DNA strands may induce strand breaks in DNA via dissociative electron attachment.[4−29]

Based on the results of computational studies (DFT level) of the sugar−phosphate−sugar model, Li et al.[7] proposed a mechanism for the LEE induced DNA single strand breakage. In this mechanism the near 0 eV energy electron may be captured first by the phosphate group, forming a phosphate-centered radical anion. This is then followed by the subsequent $C_{3'}-O_{3'}$ or $C_{5'}-O_{5'}$ σ bond breaking (with an energy barrier of about 10 kcal/mol). However, other theoretical studies[8] suggested that electrons with kinetic energies near 0 eV cannot attach directly at a significant rate to the phosphate units due to its near zero electron affinity (0.033 eV[7]). Low energy electrons should be trapped by the pyrimidine bases (with electron affinities of 0.2−0.3 eV[30,31]) rather than in the phosphate group of DNA. Along with the evidence from experiments exploring the base-releasing process of pyrimidine nucleosides,[9,10] the DFT investigations of the electron attachment to the nucleosides[11] and of the base-releasing mechanisms of the nucleosides complexes[12,13] have suggested that, in the formation of an electronically stable radical anion, the excess electron resides on the π^* orbital of pyrimidine.

These investigations have been recently expanded and new results on pyrimidine nucleotides (2′-deoxycytidine-3′-monophosphate and 2′-deoxythymidine-3′-monophosphate molecule)[9,13−17] concluded that the very low energy electron can attach to the π^* orbitals of the DNA bases. Such a process facilitates $C_{3'}-O_{3'}$ bond cleavage in an aqueous solution[13−17] This conclusion has been extended to the gas phase by the subsequent comprehensive DFT studies of additional pyrimidine nucleotides (2′-deoxycytidine-3′-monophosphate, 2′-deoxythymidine-3′-monophosphate, 2′-deoxycytidine-5′-monophosphate, and 2′-deoxythymidine-5′-monophosphate molecules). The density functional

Received: August 14, 2011
Revised: October 26, 2011
Published: October 31, 2011

theory investigations of low energy electron attachment-induced C−O σ bond breaking of pyrimidine nucleotides based on 2′-deoxycytidine-5′-monophosphate, 2′-deoxythymidine-5′-monophosphate,[18,19] 2′-deoxycytidine-3′-monophosphate, and 2′-deoxythymidine-3′-monophosphate[20] models suggested that the first step of the mechanism of the LEE induced single strand bond breaking in DNA involves the attachment of an electron to the pyrimidine bases of DNA. It is followed by formation of base-centered radical anions. Subsequently, these radical anions undergo C−O bond breaking, yielding neutral ribose radical fragments and the corresponding phosphoric anions. The $C_{3'}-O_{3'}$ bond cleavage is expected to dominate because of its low activation energy.

Investigations on the purine nucleotide models have not been so commonly carried out and much less reported. This is partly because of the negative or small electron affinities of guanine and adenine involved complexes. However, evidence suggesting the importance of guanine in capturing LEE have been accumulated. Ray et al. showed experimentally that the low energy electrons are ready to attach to the short single-stranded guanine-rich oligomers.[21] Sanche's group observed the significant contributions of guanine in the LEE-induced DNA single-strands breaking.[22] Based on the results of high level calculations, Schaefer et al. predicted substantial electron capture ability of the 2′-deoxyguanosine-3′,5′-diphosphate in both gas phase and aqueous solutions.[23] Schyman et al., applying 2′-deoxyguanosine-3′monophosphate as a model, evaluated the activation energy barrier of the $C_{3'}-O_{3'}$ bond cleavage of the electron attached-2′-deoxyguanosine-3′monophosphate to be around 10 kcal/mol in the gas phase and around 5 kcal/mol in aqueous solutions.[24] Recently, theoretical investigations of the LEE attachment induced C′−O σ bonds and *N*-glycosidic bond breaking of 2′-deoxyguanosine-3′,5′-diphosphate (3′,5′-dGDP) were performed by using the B3LYP/DZP++ approach.[25] The results reveal possibly reaction pathways in the gas phase and in aqueous solutions. It was concluded that, especially, the solvent−solute interactions greatly reduce the activation barriers of the C−O bond cleavage to 1.06−3.56 kcal/mol. Such low energy barriers ensure either $C_{5'}-O_{5'}$ or $C_{3'}-O_{3'}$ bond rupture to take place at the guanosine site in DNA single strands in aqueous solutions. These findings clearly elucidate the femtosecond time-resolved laser spectroscopic observations that the damage of dGMP dominates the electron attachment induced dissociation of nucleotides in aqueous solutions.[32]

On the other hand, studies of the LEE-induced adenine related DNA bond breaking are scarce. As far as we know the only report is the base-releasing mechanisms of the adenosine published by Li et al.[17] To advance and supplement the previous studies of guanine, thymidine, and cytidine related DNA fragments, here, we report the investigations of the reaction pathways of the LEE-induced adenine related DNA bond breaking. 2′-Deoxyadenosine-3′,5′-diphosphate (3′,5′-dADP) has been selected as a suitable model which allows us to examine both $C_{5'}-O_{5'}$ and $C_{3'}-O_{3'}$ bond cleavages (and glycosidic bond rupture) at the same time. For a better description of the influence of the 3′-5′ phosphodiester linkage in DNA, the $-OPO_3H$ moiety was terminated with CH_3 group; see Figure 1. This model complements the previous studies of the 3′,5′-diphosphate ester of the 2′-deoxyribonucleosides of guanine, thymidine, and cytidine. It provides information directly related to the important building blocks of DNA. The model used in this study represents situations in which counterions such as the Na^+ and K^+ cations are closely bound to the phosphate group of DNA. Although this model is not always exact for the aqueous solutions, it is most likely to well mimic the experiment of LEE-induced bond breaks in the thin solid films.[21]

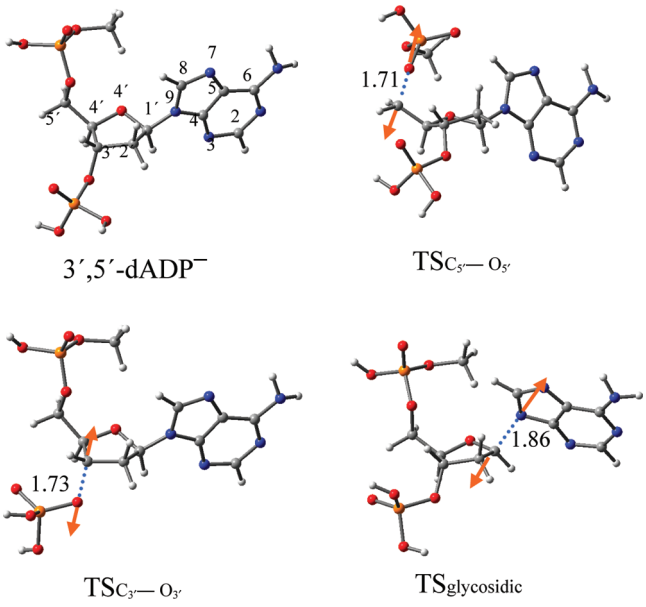

Figure 1. Optimized structures of the radical anion of 2′-deoxyguanosine-3′,5′-diphosphate (3′,5′-dADP$^-$) and the transition state structures of the $C_{5'}-O_{5'}$ bond breaking ($TSC_{5'}-O_{5'}$), $C_{3'}-O_{3'}$ bond breaking ($TSC_{3'}-O_{3'}$), and *N*-glycosidic bond breaking (TSglycosidic). Atomic distances are in Å. Orange arrows in the transition states represent the single imaginary frequency related vibration mode. Color representations: red for oxygen, gray for carbon, blue for nitrogen, orange for phosphorus, and white for hydrogen.

METHODS

Although the second order perturbation theory (MP2) has been widely used to the study of DNA subunits, this method may not be suitable for the gas phase investigation of the phenomena that are the focus of this work. The negative values predicted at the MP2 level of theory for electron affinity of the pyrimidine nucleotides in the gas phase[8,14,15] are inconsistent with experimental results on DNA[30] and RNA[33] fragments and higher-level theoretical investigations. Both experiments and higher-level theoretical investigations indicate unambiguously the positive electron affinities for the pyrimidine bases, the pyrimidine nucleosides, and the pyrimidine nucleotides in the gas phase[11,12,27,31] On the other hand, the development of a comprehensive DFT bracketing technique[35] reveals the adiabatic electron affinity (EA_{ad}) values for the DNA and RNA bases consisting well with the experimental data.[30] With the reliably calibrated B3LYP/DZP++ approach, accurate calculations of the electron affinities of the 2′-deoxyribonucleosides have been accomplished.[11,35] These theoretical predictions of the electron affinities of the 2′-deoxyribonucleosides have been confirmed by the recent experiment.[36] The applied B3LYP/DZP++ approach provides a reliable description of the properties of the radical anions of the nucleotides and the accurate determination of the activation energy barrier of the corresponding bond rupture. In accord with the previous successful applications, the B3LYP/DZP++ method was also used in the present study.

Table 1. Electron Attachment and Detachment Energies (in eV)

process	EA_{ad}	VEA[a]	VDE[b]
3′,5′-dADP → 3′,5′-dADP$^-$ gas phase	0.10 (0.22)[c]	0.04[c]	0.26[c]
3′,5′-dADP → 3′,5′-dADP$^-$ PCM model	1.59[c]	1.37	1.59

[a] VAE = E(neutral) − E(anion); the energies are evaluated using the optimized neutral structures. [b] VDE = E(neutral) − E(anion); the energies are evaluated using the optimized anion structures. [c] Reference 23.

Table 2. Relative Energies of Transition States of Bond Break Pathways in the Gas Phase (kcal/mol)

bond breaking process	ΔE_{TS}[a]	ΔE^0_{TS}[b]	ΔG^0_{TS}[c]
$C_{5'}-O_{5'}$ bond	9.99	9.32	11.06
$C_{3'}-O_{3'}$ bond	8.94	7.07	7.33
N-glycosidic bond	21.29 (20.3[d])	19.99	20.99

[a] ΔE_{TS} = E(transition state) − E(radical anion). [b] With the zero point energy (ZPE) correction. [c] Free energy at T = 298 K. [d] Reference 13, using 2′-deoxyadenosine as the model.

Table 3. Relative Energies of Transition States of Bond Break Pathways in the Presence of the Polarizable Surroundings (kcal/mol)

bond breaking process	ΔE_{TS}[a]
$C_{5'}-O_{5'}$ bond	22.54
$C_{3'}-O_{3'}$ bond	13.22
N-glycosidic bond	20.91

[a] ΔE_{TS} = E(transition state) − E(radical anion); using PCM model with ε = 78.

Geometries and vibrationally zero-point corrected energies for the considered model molecules were determined using the B3LYP functional.[37,38] On the basis of the gas phase optimized geometries, the polarizable continuum model (PCM)[39] with a dielectric constant of water (ε = 78.39) was used in the calculations of the energies in a polar environment. It should be noted that this PCM model only to some extent approximates the real situation of aqueous solvation because the important effects of the microsolvation could not be included in this approach. Rather, the PCM model used in the present study accounts for the existence of the polarizable surroundings which resembles the situation in the experiment of LEE-induced bond breaks in the thin solid films.

The adiabatic electron affinity (EA_{ad}) was predicted as the difference between the total energies of the appropriate neutral and anionic species at their respective optimized geometries: $EA_{ad} = E_{neut} - E_{anion}$. The DZP++ basis sets were constructed by augmenting the Huzinaga−Dunning[40−42] set of contracted double-ζ Gaussian functions with one set of *p*-type polarization functions for each H atom and one set of five d-type polarization functions for each C, N, O, or P atom (α_p(H) = 0.75, α_d(C) = 0.75, α_d(N) = 0.80, α_d(O) = 0.85, α_d(P) = 0.60). To complete the DZP++ basis, one even-tempered diffuse *s* function was added to each H atom, while sets of even-tempered diffuse s and p functions were centered on each heavy atom. The even-tempered orbital exponents were determined according to the prescription of Lee and Schaefer.[43] The Gaussian 03 programs[44] were used in the computation.

RESULTS AND DISCUSSION

Electron Attachment to 3′,5′-dADP. The electron attachment and detachment energies of 3′,5′-dADP are summarized as follows (Table 1): the adiabatic electron affinity (EA_{ad}) of 3′,5′-dADP is 0.22 eV, the vertical attachment energy is 0.02 eV, and the vertical detachment energy (VDE) of the corresponding 3′,5′-dADP$^-$ radical anion is 0.26 eV. These values are the same as those reported in the previous work.[23]

An interaction with the polarizable surroundings (represented by water as a solvent) remarkably improves the electron capture ability of 3′,5′-dADP (EA_{ad} amounts to 1.59 eV and VEA increases to 1.37 eV in the PCM model). Moreover, due to the solvent interactions, the VDE of 3′,5′-dADP$^-$ increases up to 1.59 eV. This large VDE value implies that in the presence of the polarizable surroundings the reactions with energy barrier of less than 23 kcal/mol might occur before the electron detachment for this radical anion.

Activation Energies of the $C_{5'}-O_{5'}$ σ Bond Breaking Process in the Radical Anion of 3′,5′-dADP. To explore the potential energy surface for the $C_{5'}-O_{5'}$ σ bond cleavage process, the transition state corresponding to the $C_{5'}-O_{5'}$ σ bond association for the radical anions of 3′,5′-dADP has been located. The single imaginary vibrational frequency that characterizes this transition state amounts to 883i cm^{-1}, which is in line with those frequencies predicted in the studies of the $C_{5'}-O_{5'}$ σ bond breaking of 3′,5′-dGDP$^-$ (848i cm^{-1})[26] and of pyrimidine nucleotides (858i cm^{-1} for 5′-dCMPH$^-$ and to 758i cm^{-1} for 5′-dTMPH$^-$).[18] The elongated $C_{5'}-O_{5'}$ atomic distance of 1.714 Å and the normal mode corresponding to the imaginary vibrational frequency (Figure 1) confirm that this transition state associates with the $C_{5'}-O_{5'}$ σ bond breaking process. The activation energy of the $C_{5'}-O_{5'}$ σ bond cleavage process has been predicted to be 9.99 kcal/mol (Table 2, without the zero-point energy correction, ZPE). As a comparison, the activation energy predicted for the $C_{5'}-O_{5'}$ σ bond breaking is higher in 3′,5′-dGDP$^-$ (12.97 kcal/mol)[25] and in 5′-dCMPH$^-$ (14.3 kcal/mol) and in 5′-dTMPH$^-$ (13.8 kcal/mol).[18]

The effects of the polarizable medium raise the $C_{5'}-O_{5'}$ σ bond breaking energy barrier dramatically (22.54 kcal/mol with the PCM model prediction, Table 3) in 3′,5′-dADP$^-$. This substantial increase compares to the cases of pyrimidine nucleotides, in which the effects of the polarizable surroundings raise the $C_{5'}-O_{5'}$ σ bond breaking energy barrier up to 18.0 kcal/mol for 5′-dCMPH$^-$ and to 17.9 kcal/mol for 5′-dTMPH$^-$.[18] On the other hand, the influence of the polarizable medium greatly decreases the $C_{5'}-O_{5'}$ σ bond breaking energy barrier in 3′,5′-dGDP$^-$. These opposite effects could be partly correlated to the dipole moment variations (1.80 D for 3′,5′-dADP$^-$ and 19.8 D for 3′,5′-dGDP$^-$[25]) induced by the solvent−solute interaction at the transition state corresponding to the $C_{5'}-O_{5'}$ σ bond rupture.

Activation Energies of the $C_{3'}-O_{3'}$ σ Bond Breaking Process in the Radical Anion of 3′,5′-dADP. The transition state for the $C_{3'}-O_{3'}$ σ bond cleavage process in the radical anion of 3′,5′-dADP has been located and characterized by the single imaginary vibrational frequency. The elongated $C_{3'}-O_{3'}$ atomic distance (1.733 Å) and the normal mode corresponding to the imaginary vibrational frequency characterize the $C_{3'}-O_{3'}$ σ bond breaking process (Figure 1). The activation energy of the

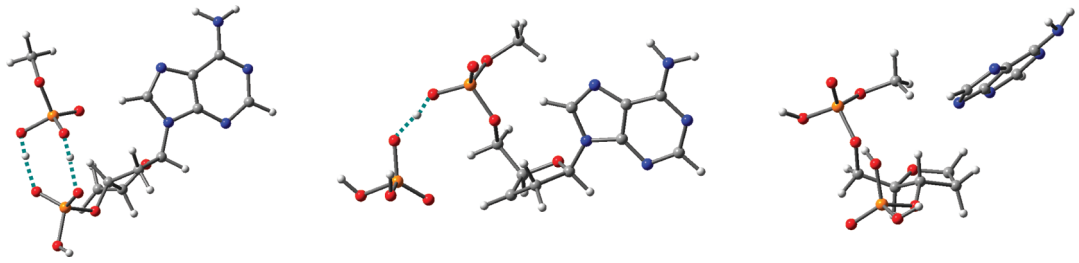

Figure 2. Optimized structures of the bond-broken product: $C_{5'}-O_{5'}$ bond broken ($PC_{5'}-O_{5'}$), $C_{3'}-O_{3'}$ bond broken ($PC_{3'}-O_{3'}$), and *N*-glycosidic bond broken (Pglycosidic).

Table 4. Relative Energies of the Bond Broken Products (kcal/mol)

bond breaking process	ΔE^a	$\Delta E_{PCM}{}^b$
$C_{5'}-O_{5'}$ bond	−54.09	−38.13
$C_{3'}-O_{3'}$ bond	−45.25	−36.22
N-glycosidic bond	−9.36	−0.89

[a] $\Delta E = E$(bond broken product) − E(radical anion). [b] $\Delta E_{PCM} = E$(bond broken product) − E(radical anion); using PCM model with $\varepsilon = 78$.

$C_{3'}-O_{3'}$ σ bond breaking has been predicted to be 8.94 kcal/mol (Table 2, without ZPE). This energy barrier is about 2 kcal/mol smaller than in the corresponding guanosine complexes (11.23 kcal/mol for the 3′,5′-dGDP model[26] and 10.28 kcal/mol for the 3′-dGMP model[25]). As a comparison, the activation energy needed for the $C_{3'}-O_{3'}$ σ bond breaking in pyrimidine nucleotides is even lower in 3′-dCMPH$^-$ (6.2 kcal/mol) and in 3′-dTMPH$^-$ (7.1 kcal/mol),[18] owing to the SN2-like reaction mechanism.

Similar to the process of the $C_{5'}-O_{5'}$ σ bond rupture, the effects of the polarizable surroundings increase significantly the energy barrier of the $C_{3'}-O_{3'}$ σ bond rupture in 3′,5′-dADP$^-$ (13.22 kcal/mol with the PCM model prediction). This effect can also be seen in the 3′-dCMP and the 3′-dTMP model (12.82 kcal/mol for 3′-dCDP$^-$ and 13.73 kcal/mol for 3′-dTDP$^-$).[18]

Activation Energies of the *N*-Glycosidic Bond Breaking Process in the Radical Anion of 3′,5′-dADP. The transition state for *N*-glycosidic bond breaking of the radical anion of 3′,5′-dADP has been located and characterized by the elongated $C_{1'}-N_9$ atomic distance (1.861 Å). This is further confirmed by the existence of single imaginary vibrational frequency of 621i cm^{-1} and the corresponding normal mode representing the $C_{1'}-N_9$ σ bond breaking (Figure 1). The activation energy of the $C_{1'}-N_9$ glycosidic bond breaking has been predicted to be 21.29 kcal/mol (Table 2, without ZPE). On the basis of the nucleoside model, this bond rupture energy barrier is predicted to be 20.3 kcal/mol. The existence of the neighboring phosphates on the ribose moiety slightly increases the energy barrier. Moreover, this energy barrier is also close to that reported in the previous studies on the LEE induced glycosidic bond cleavage in pyrimidine nucleosides, in which the activation energy was predicted to be 18.9−21.6 kcal/mol for the C−N bond beak.[12,13] For further comparison, note that the activation energy for the glycosidic bond cleavage in 3′,5′-dGDP$^-$ is considerably higher (24.08 kcal/mol).[25]

Contrary to the C−O σ bond rupture, the polarizable surroundings barely influence the energy barrier of the *N*-glycosidic bond breaking (20.91 kcal/mol for 3′,5′-dADP$^-$ in the presence of the polarizable surroundings).

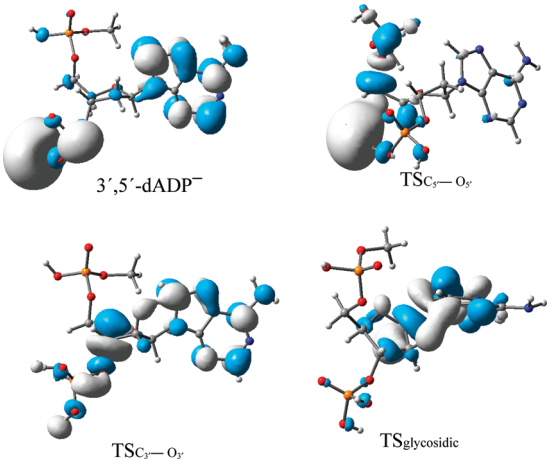

Figure 3. SOMOs of radical anion of 2′-deoxyadenosine-3′,5′-diphosphate (3′,5′-dADP$^-$) and the transition states of the $C_{5'}-O_{5'}$ bond breaking ($TSC_{5'}-O_{5'}$), $C_{3'}-O_{3'}$ bond breaking ($TSC_{3'}-O_{3'}$), and *N*-glycosidic bond breaking (TSglycosidic) in the gas phase. The typical characteristics of the σ antibond orbital of the breaking bond are shown clearly.

Products of the C−O σ Bonds and *N*-Glycosidic Bond Breaking Processes of the Radical Anion of 3′,5′-dADP. Both $C_{3'}-O_{3'}$ and $C_{5'}-O_{5'}$ σ bond ruptures lead to the energetically stable complexes consisting of a phosphate anion and a corresponding carbon-centered neutral radical (Figure 2). In the former case, the $C_{5'}-O_{5'}$ σ bond breaking product is by 54.09 kcal/mol more stable than 3′,5′-dADP$^-$ (Table 4). Meanwhile, the energy of the $C_{3'}-O_{3'}$ σ bond breaking product is 45.25 kcal/mol lower than that of 3′,5′-dADP$^-$. The formation of two H-bonds between the phosphate groups in the $C_{5'}-O_{5'}$ σ bond breaking product is the reason for this energy difference between these two C−O σ type bond breaking products. However, solvent effects destabilize these products by about 16 kcal/mol (9 kcal/mol for the $C_{3'}-O_{3'}$ σ bond breaking product). Thus, the polarizable surroundings seem to less influence these intra H-bonded complexes.

N-Glycosidic bond breaking product in the gas phase is about 9.36 kcal/mol lower than in the case of 3′,5′-dADP$^-$. In the gas phase this complex contains a deprotonated adenine anion and a ribose-centered phosphate−sugar−phosphate radical. In the presence of the polarizable surroundings, this *N*-glycosidic bond breaking product is significantly destabilized by the surrounding−solute interactions. The total energy of this complex is only about 0.89 kcal/mol lower than that of 3′,5′-dADP$^-$.

Molecular Orbital Analysis. The characteristics of singly occupied molecular orbitals (SOMO) shed light on the electron

attachment and the bond breaking mechanisms. Figure 3 displays the distribution of the unpaired electron along the LEE-induced bond breaking pathways of 3′,5′-dADP. In the gas phase, the SOMO of 3′,5′-dADP$^-$ indicates that the excess electron is partly covalently bonded to the 3′-phosphate and partly covalently bonded to the adenine base moiety (Figure 3).

One of the critical characteristics revealed in the previous studies of the LEE-induced bond dissociation in the pyrimidine related nucleotides is that the excess negative charge is partly located on the bond to be damaged.[14] The SOMO of the transition states in Figure 3 exhibits the similar characteristics of the charge-induced bond dissociation. The antibonding orbital of the $C_{5'}-O_{5'}$ bond can be recognized clearly in the SOMO of the transition state corresponding to the $C_{5'}-O_{5'}$ σ bond rupture. Meanwhile, the antibonding feature of the $C_{3'}-O_{3'}$ bond is obvious in the SOMO representing the transition state of the $C_{3'}-O_{3'}$ σ bond rupture. Similarly, the partial occupation of the *N*-glycosidic antibonding MO and partial occupation of the π^* orbital of the guanine moiety is shown in the SOMO of the transition state corresponding to the *N*-glycosidic bond damage. It should be noted that the unpaired electron is partly distributed on the base moiety in the transition state of the $C_{3'}-O_{3'}$ σ bond rupture, whereas it is partly located on the phosphate group at 3′-position in the transition state of the $C_{5'}-O_{5'}$ σ bond rupture. These two different distributions are responsible for the relative low activation energy of the σ bond cleavages.

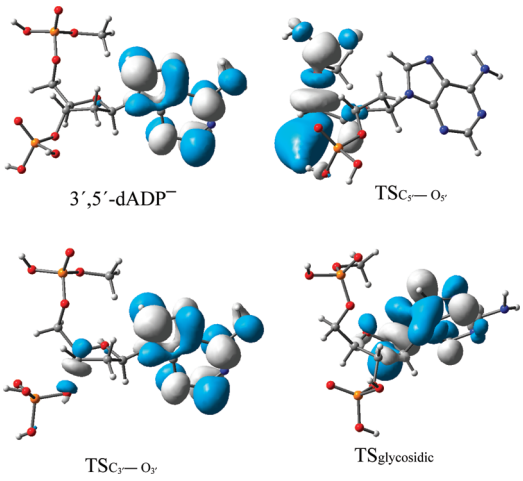

Figure 4. SOMOs of radical anion of 2′-deoxyadenosine-3′,5′-diphosphate (3′,5′-dADP$^-$) and the transition states of the $C_{5'}-O_{5'}$ bond breaking ($TSC_{5'}-O_{5'}$), $C_{3'}-O_{3'}$ bond breaking ($TSC_{3'}-O_{3'}$), and *N*-glycosidic bond breaking (TSglycosidic) in the presence of the polarizable surroundings.

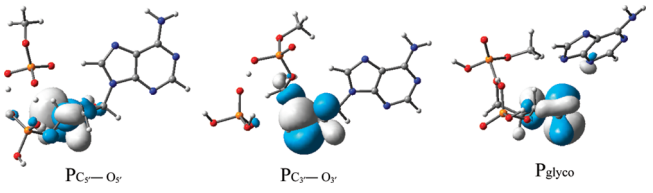

Figure 5. SOMOs of the bond-broken products: $PC_{5'}-O_{5'}$, $PC_{3'}-O_{3'}$, and Pglycosidic in the gas phase.

The SOMO of the C−O bond breaking products confirms that the radical resides on the C5′ of the 2′-deoxyadenosine-C5′(*HH*′)-yl-3′-monophosphate in $C_{5'}-O_{5'}$ σ bond rupture product and on the C3′ of the 2′-deoxyadenosine-C3′(*H*)-yl-5′-monophosphate in $C_{3'}-O_{3'}$ σ bond breaking product. The SOMO characteristics of the *N*-glycosidic bond dissociation product in gas phase indicate that the radical is located at the C1′-position of the ribose moiety .

The main influence of the solvent effects on the distribution of the excess electron in the radicals is elimination of the partial dipole-bounded characteristics shown in the gas phase. In the presence of the polarizable surroundings, the SOMO of 3′,5′-dADP$^-$ indicates that the excess electron is mainly covalently bonded to the base moiety (Figure 4). It is interesting to note that the unpaired excess electron is mainly located on the base portion in the transition states of the $C_{3'}-O_{3'}$ σ bond rupture. This might be related to the fact that the $C_{3'}-O_{3'}$ σ bond rupture has the lowest activation energy barrier.

Reaction Pathways of the LEE-Induced DNA Single Strands. The low energy electron-induced single strand bond breaking in the adenine-rich DNA might take place the same way as that of the pyrimidines: the electrons partly bound to the base group, forming an adenine-centered radical anion of the nucleotide. Subsequently, this radical anion undergoes the C−O bond or glycosidic bond breaking and yield corresponding radical fragments and anions.

In the gas phase, the glycosidic bond breaking requires activation energy as high as 21.28 kcal/mol. Therefore, base release should be excluded, based on the energy consideration. The energy barrier for the $C_{3'}-O_{3'}$ σ bond cleavage process (8.94 kcal/mol) is close to that of $C_{5'}-O_{5'}$ σ bond cleavage process (9.99 kcal/mol). Both pathways seem to be compatible. However, relatively small electron vertical detachment energy

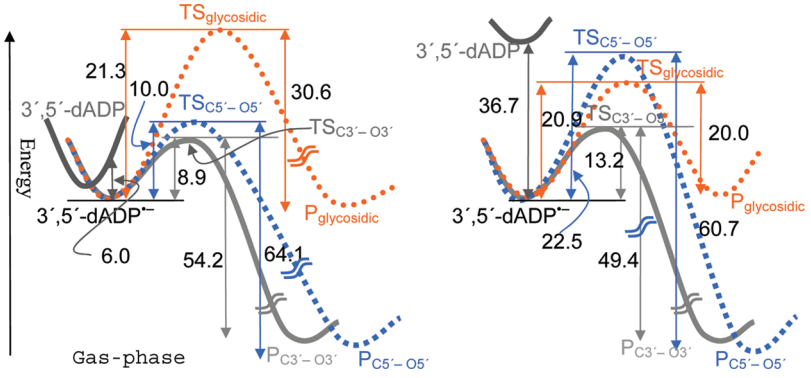

Figure 6. Energy profile of the $C_{5'}-O_{5'}$, $C_{3'}-O_{3'}$, and *N*-glycosidic bond breaking process in the gas phase and in the presence of the polarizable surroundings.

dx.doi.org/10.1021/jp207801e |*J. Phys. Chem. B* 2011, 115, 14831–14837

(VDE = 0.26 eV or 6.00 kcal/mol) of the corresponding radical anion 3′,5′-dADP$^-$ suggests that electron detachment should dominate in the gas phase. Therefore, the LEE attachment is unlikely to directly induce the strand breaks at the adenine site in the DNA single strands.

An application of the PCM model to represent the effects of the polarizable surroundings implies that there is no proton transfer or charge transfer between solute and solvent considered. In this approximation, the effects of the polarizable surroundings not only greatly increase the activation energies of the C−O σ bond cleavage processes (13.22 kcal/mol for $C_{3'}-O_{3'}$ σ bond rupture and 22.54 kcal/mol for $C_{5'}-O_{5'}$ σ bond rupture) but also significantly increase the electron vertical detachment energy (VDE = 1.59 eV or 36.69 kcal/mol) of 3′,5′-dADP$^-$. Consequently, $C_{3'}-O_{3'}$ σ bond rupture is expected to be able to occur for the adenine-centered radical anion in the presence of polarizable medium. Considering that the presence of the polarizable surroundings hardly changes the activation energy barrier of N-glycosidic bond breaking, $C_{3'}-O_{3'}$ σ bond cleavage processes should dominate the LEE induced DNA single strand dissociation in the adenine-rich DNA (Figure 6).

CONCLUSIONS

The results of our study along with the findings of the earlier investigations[13,24] indicate that although adenine-rich oligonucleotides are capable of capturing the near 0 eV electron to form the electronically stable radical anions in the gas phase they are unlikely to undergo either C−O σ bond cleavage or the glycosidic processes due to the low electron detachment energy of 3′,5′-dADP$^-$ unit (0.26 eV). Instead, these radical anions should directly yield an electron detachment product in the gas phase. This situation is similar in the 3′,5′-dGDP$^-$ model study, in which the relatively small VDE of the radical anion of guansine-3′,5′-diphosphoric acid in the gas phase suggests that electron detachment should dominate the subsequent reactions. Therefore, in the gas phase the most possible location for the LEE attachment-induced DNA single strand breaking should occur around the pyrimidine sites.

In the presence of polarizable surroundings, due to the great increase of the electron detachment energy (VDE increases to 1.59 eV), the adenine-centered radical anions could directly lead to strand breaks in the adenine-rich DNA single strands through either σ bond or *N*-glycosidic bond breaking. However, due to the much higher activation energy for rupture of the $C_{5'}-O_{5'}$ σ bond (22.54 kcal/mol) and for the *N*-glycosidic bond (20.19 kcal/mol), the $C_{3'}-O_{3'}$ σ bond breaking should be the only possible pathway. Moreover, as revealed in the previous study of the 3′,5′-dGDP$^-$ model, in the presence of the polarizable surroundings, the significant low activation barriers of the C−O bond cleavage (1.1−3.6 kcal/mol) ensure that the C−O bond breakings at the guanosine sites suppress over those at the adenine sites in the bond ruptures of DNA single strands.

It is important to note that, in the PCM calculations, the predicted ratio of the activation energy barrier of the $C_{5'}-O_{5'}$ σ bond breakage in the 3′,5′-dXDP$^-$ (X = G, A, T) amounts to 1.1:22.54:18.75. This ratio partly explain the observation in the femtosecond time-resolved laser spectroscopic experiment[33] that the $C_{5'}-O_{5'}$ σ bond breaking only occurs in dGMP$^-$ and dTMP$^-$ not in dAMP$^-$. It should be noted that previous studies have indicated that the radical anion of dCMP is ready to accept a proton to form a stable neutral radical species (dCHMP) from the neighboring proton donors, therefore, the theoretical models 5′-dCMP$^-$ and 3′,5′-dCDP$^-$ could not be used to elucidate the experiments in aqueous solutions.

In summary, in combination with the previous investigations, this study completes the LEE-induced DNA single strand breaking computational research for the four basic DNA units 3′,5′-dXDP (X = G, A, T, C). The obtained results are valuable for elucidating the experimental observations. The information revealed in this series of studies sheds a light on mechanisms of the interactions between the LEE and the DNA stands.

AUTHOR INFORMATION

Corresponding Author

*E-mail: jiande@icnanotox.org (J.G.); jerzy@icnanotox.org (J.L.).

ACKNOWLEDGMENT

This project in the U.S.A. was supported by the NSF CREST Grant No. HRD-0833178. In China it was supported by National Science & Technology Major Project "Key New Drug Creation and Manufacturing Program", China (Number: 2009ZX09301-001). We thank the Mississippi Center for Supercomputing Research for a generous allotment of computer time.

REFERENCES

(1) Boudaiffa, B.; Cloutier, P.; Hunting, D.; Huels, M. A.; Sanche, L. *Science* **2000**, *287*, 1658–1660.
(2) LaVerne, J. A.; Pimblott, S. M. *Radiat. Res.* **1995**, *141*, 208–215.
(3) Pimblott, S. M. LaVerne, J. A. In *Radiation Damage in DNA: Structure/Function Relationships at Early Times*; Fuciarelli, A. F., Zimbrick, J. D., Eds.; Battelle: Columbus, OH, 1995; pp 3−12.
(4) Pan, X.; Cloutier, P.; Hunting, D.; Sanche, L. *Phys. Rev. Lett.* **2003**, *90*, 208102−1–208102−4.
(5) Caron, L. G.; Sanche, L. *Phys. Rev. Lett.* **2003**, *91*, 113201.
(6) Huels, M. A.; Boudaiffa, B.; Cloutier, P.; Hunting, D.; Sanche, L. *J. Am. Chem. Soc.* **2003**, *125*, 4467–4477.
(7) Li, X.; Sevilla, M. D.; Sanche, L. *J. Am. Chem. Soc.* **2003**, *125*, 13668–13669.
(8) Berdys, J.; Anusiewicz, I.; Skurski, P.; Simons, J. *J. Am. Chem. Soc.* **2004**, *126*, 6441–6447.
(9) Zheng, Y.; Cloutier, P.; Hunting, D.; Wagner, J. R.; Sanche, L. *J. Am. Chem. Soc.* **2004**, *126*, 1002–1003.
(10) Abdoul-Carime, H.; Gohlke, S.; Fischbach, E.; Scheike, J.; Illenberger, E. *Chem. Phys. Lett.* **2004**, *387*, 267–270.
(11) Richardson, N. A.; Gu, J.; Wang, S.; Xie, Y.; Schaefer, H. F. *J. Am. Chem. Soc.* **2004**, *126*, 4404–4411.
(12) Gu, J.; Xie, Y.; Schaefer, H. F. *J. Am. Chem. Soc.* **2005**, *127*, 1053–1057.
(13) Li, X.; Sanche, L.; Sevilla, M. D. *Radiat. Res.* **2006**, *165*, 721–729.
(14) Barrios, R.; Skurski, P.; Simons, J. *J. Phys. Chem. B* **2002**, *106*, 7991–7994.
(15) Berdys, J.; Skurski, P.; Simons, J. *J. Phys. Chem. B* **2004**, *108*, 5800–5805.
(16) Berdys, J.; Anusiewicz, I.; Skurski, P.; Simons, J. *J. Phys. Chem. A* **2004**, *108*, 2999–3005.
(17) Simons, J. *Acc. Chem. Res.* **2006**, *39*, 772–779.
(18) Bao, X.; Wang, J.; Gu, J.; Leszczynski, J. *Proc. Natl. Acad. Sci. U.S.A.* **2006**, *103*, 5658–5663.
(19) Kumar, A.; Sevilla, M. D. *J. Phys. Chem. B* **2007**, *111*, 5464–5474.
(20) Gu, J.; Wang, J.; Leszczynski, J. *J. Am. Chem. Soc.* **2006**, *128*, 9322–9323.

(21) Ray, S. G.; Daube, S. S.; Naaman, R. *Proc. Natl. Acad. Sci. U.S.A.* **2006**, *102*, 15–19.
(22) Zheng, Y.; Cloutier, P.; Hunting, D. J.; Sanche, L.; Wagner, J. R. *J. Am. Chem. Soc.* **2005**, *127*, 16592–16598.
(23) Gu, J.; Xie, Y.; Schaefer, H. F. *Nucleic Acids Res.* **2007**, *35*, 5165–5172.
(24) Schyman, P.; Laaksonen, A. *J. Am. Chem. Soc.* **2008**, *130*, 12254–12255.
(25) Gu, J.; Wang, J.; Leszczynski, J. *ChemPhysChem* **2010**, *11*, 175–181.
(26) Sanche, L. *Eur. Phys. J. D* **2005**, *35*, 367–390.
(27) Gu, J.; Xie, Y.; Schaefer, H. F. *J. Am. Chem. Soc.* **2006**, *128*, 1250–1252.
(28) Martin, F.; Burrow, P. D.; Cai, Z.; Cloutier, P.; Hunting, D.; Sanche, L. *Phys. Rev. Lett.* **2004**, *93*, 068101−1–068101−4.
(29) Zheng, Y.; Cloutier, P.; Hunting, D. J.; Wagner, J. R.; Sanche, L. *J. Chem. Phys.* **2006**, *124*, 064710.
(30) Schiedt, J.; Weinkauf, R.; Neumark, D. M.; Schlag, E. W. *Chem. Phys.* **1998**, *239*, 511–524.
(31) Wesolowski, S. S.; Leininger, M. L.; Pentchev, P. N.; Schaefer, H. F. *J. Am. Chem. Soc.* **2001**, *123*, 4023–4028.
(32) Wang, C. R.; Nguyen, J.; Lu, Q. B. *J. Am. Chem. Soc.* **2009**, *131*, 11320–11322.
(33) Hanel, G.; Gstir, B.; Denifl, S.; Scheier, P.; Probst, M.; Farizon, B.; Farizon, M.; Illenberger, E.; Mark, T. D. *Phys. Rev. Lett.* **2003**, *90*, 188104−1–188104−4.
(34) Rienstra-Kiracofe, J. C.; Tschumper, G. S.; Schaefer, H. F.; Nandi, S.; Ellison, G. B. *Chem. Rev.* **2002**, *102*, 231–282.
(35) Gu, J.; Xie, Y.; Schaefer, H. F. *J. Phys. Chem. B* **2005**, *109*, 13067–13075.
(36) Stokes, S. T.; Li, X.; Grubisic, A.; Ko, Y. J.; Bowen, K. H. *J. Chem. Phys.* **2007**, *127*, 084321−6.
(37) Becke, A. D. *J. Chem. Phys.* **1993**, *98*, 5648–5652.
(38) Lee, C.; Yang, W.; Parr, R. G. *Phys. Rev. B* **1988**, *37*, 785–789.
(39) Cossi, M.; Barone, V.; Cammi, R.; Tomasi, J. *Chem. Phys. Lett.* **1996**, *255*, 327–335.
(40) Huzinaga, S. *J. Chem. Phys.* **1965**, *42*, 1293–1302.
(41) Dunning, T. H. *J. Chem. Phys.* **1970**, *53*, 2823–2833.
(42) Dunning, T. H.; Hay, P. J. In *Modern Theoretical Chemistry*; Schaefer, H. F., Ed.; Plenum Press: New York, 1977; Vol. 3, pp 1−27.
(43) Lee, T. J.; Schaefer, H. F. *J. Chem. Phys.* **1985**, *83*, 1784–1794.
(44) Frisch, M. J.; et al. *Gaussian 09*, revision A.1; Gaussian, Inc.: Wallingford, CT, 2009.